

Changes in Tropospheric Ozone Associated With Strong Earthquakes and Possible Mechanism

Feng Jing , *Member, IEEE*, and Ramesh P. Singh , *Senior Member, IEEE*

Abstract—The index of ozone anomaly (IOA) has been proposed to detect changes in tropospheric ozone associated with strong earthquakes. The tropospheric ozone prior and after the 2008 Wenchuan earthquake has been analyzed using IOA. Atmospheric infrared sounder ozone volume mixing ratio (O₃ VMR) at different pressure levels (600, 500, 400, 300, 200 hPa) for an 18-year period 2003–2020 has been considered to identify the unique behavior associated with the strong earthquakes. Our results show distinct enhancement in tropospheric ozone occurred 5 d (7 May 2008) prior to the main event and distributed along the Longmenshan fault zone. An enhancement in IOA has also been observed around the time of the 2013 Lushan and 2017 Jiuzhaigou earthquakes, but with the different emergence time, which indicates that the unusual behavior of tropospheric ozone depends on the tectonic and geological environment, focal mechanism, focal depth, meteorological conditions, and other factors. The location of increased tropospheric ozone indicates the epicenter of earthquakes. The magnitude of earthquake could be one of the important factors affecting the appearance of the anomalous tropospheric ozone. The possible mechanism for the increased tropospheric ozone associated with strong earthquakes is discussed in this article. The quasi-synchronous changes of tropospheric ozone and other parameters in the lithosphere/atmosphere/ionosphere have been found by combining with the other published results related to the Wenchuan earthquake, which show the existence of coupling during the earthquake preparation phase associated with the lithosphere–atmosphere–ionosphere coupling.

Index Terms—Earthquakes, lithosphere–atmosphere–ionosphere coupling (LAIC) model, tropospheric ozone, Wenchuan earthquake.

I. INTRODUCTION

THE EARTHQUAKE is a complex process within preparation region. Within the stress built up region, slow deformation takes place that leads to the unusual geochemical, geophysical, hydrological signals, and greenhouse gas emissions, which have been observed using borehole, ground, and satellite observations [3]–[7]. These observations have provided changes in meteorological, atmospheric and ionospheric parameters, which were reported by many associated with earthquakes

occurred globally [9], [10]. The changes observed in borehole, ground, atmospheric, and ionospheric parameters have provided evidence to believe existence of strong coupling between land–atmosphere–ionosphere during the phase of earthquake preparation [11]–[13]. The optical and microwave satellite observations have provided anomalous signals associated with tectonic and seismic activities, which encouraged us to explore the coupling of multi-parameter to get an early information about an impending earthquake [14]–[16]. In the past three decades, the short-term signals observed by satellite for thermal radiation [17]–[19], gas emission [5], [20], [21], atmospheric aerosol [22], [23], and ionospheric disturbances [24]–[26] associated with the different earthquakes around the world. The models of lithosphere–atmosphere–ionosphere coupling (LAIC) [28], [29] and lithosphere–coversphere–atmosphere coupling [8] have been proposed to understand the earthquake processes and associated anomalous variations.

Ozone (O₃) is one of the most important trace gases in the atmosphere, and the stratosphere is considered as home of the ozone. Changes in the total ozone column (TOC) have been observed globally, which are associated with seasonal changes, dust storms [30], tropospheric–stratospheric exchanges, weather disturbances, volcanic eruptions [31], atmospheric disturbances, and cyclone/hurricanes. Lasukov [32] proposed ozone production associated with the rock deformation and fracture growth as the electromagnetic wave propagates from the hypocentral region to ionosphere, the anomalous electromagnetic signals reflecting changes in ionosphere provide a potential early warning signal about an impending earthquake. The analysis of ozone data observed by satellite shows decline in TOC occurred on the day of earthquake [34], [35], which was thought to be easier to observe during spring season due to convection and exchanges between troposphere–stratosphere [38]. The increased TOC have been observed a few days (even 7 d) prior [39], [40] and after the earthquake [15], [41], that could be associated with the transportation from higher latitude in the troposphere and the intrusion of stratospheric ozone [41]. Xiong *et al.* [44] used machine learning and global earthquakes to verify the anomaly of ozone before earthquakes. But some other researchers claimed that there are no statistically significant TOC variations and earthquake activities [45]–[47].

Besides these possible stratospheric ozone variabilities associated with the earthquakes, Baragiola *et al.* [48] provided the experimental evidence for the generation of tropospheric ozone during rock fracture due to large electric fields induced by

Manuscript received January 22, 2021; revised March 20, 2021; accepted May 10, 2021. Date of publication May 17, 2021; date of current version June 8, 2021. This work was supported in part by the National Natural Science Foundation of China under Grant 42074082, Grant 41604062, and Grant 41774111, and in part by the APSCO Earthquake Research Project Phase II: Integrating Satellite and Ground Observations for Earthquake Signatures and Precursors. (Corresponding author: Ramesh P. Singh.)

Feng Jing is with the Institute of Earthquake Forecasting, China Earthquake Administration, Beijing 100036, China (e-mail: jingfeng@cea-ies.ac.cn).

Ramesh P. Singh is with the Schmid College of Science and Technology, Chapman University, Orange, CA 92866 USA (e-mail: rsingh@chapman.edu). Digital Object Identifier 10.1109/JSTARS.2021.3080843

charge separation. But their results did not support the TOC variations because the content of tropospheric ozone is very lower compared with the stratospheric ozone. The tropospheric ozone is associated with the photochemical and chemical reactions, which depends on sunlight (especially ultraviolet light) and ozone precursors, i.e., hydrocarbons (e.g., methane), nitrogen oxides (NO_x), CO, and volatile organic compounds (VOCs) originated from natural and man-made sources, and also could be due to downward migration from stratosphere through diffusion and turbulence processes [49], [50]. But such observations have motivated earthquake community to study if the ozone can prove to be an earthquake precursor.¹

In the present study, we have considered ozone data for an 18-year period (2003 to 2020) observed by the atmospheric infrared sounder (AIRS) onboard the earth observing system (EOS) Aqua satellite to study the possible relationship between the tropospheric ozone variations and the strong earthquakes. The 2008 Wenchuan earthquake occurred in Sichuan province of China was selected as a case due to the extensive research by the scientific community. Our results show that an enhancement in tropospheric ozone over the epicentral area 5 d prior to the main earthquake event, which could be a unique behavior in both temporal and spatial domains. The quasi-synchronous changes in the tropospheric ozone and other parameters at different vertical altitudes (lithosphere, atmosphere, and ionosphere) indicate the existence of coupling effect during the earthquake preparation phase.

II. DATA AND METHOD

A. Data Used

The daily Level 3 products AIRS3STD (L3 daily gridded standard retrieval product using AIRS IR-Only) and AIRS3STM (L3 monthly gridded standard retrieval product using AIRS IR-Only) with the spatial resolution of 1.0° 1.0° have been used in the present work. The retrieval algorithm and quality control related to the version 6 AIRS data products can be found in [51] and [52]. Ozone volume mixing ratio (O3 VMR) at different pressure levels have been considered in order to obtain the possible variation triggered by tectonic and seismic activities. Only the nighttime data have been considered in order to reduce the interferences coming from human activities and solar radiation during daytime. OMI/Aura Level-3 daily nitrogen dioxide (NO₂) global gridded product (OMNO2d) with the spatial resolution of 0.25° 0.25° is considered since it is an important tropospheric ozone precursor.

B. Methods

The emergence of geophysical, hydrological, and geochemical anomalies prior to earthquake activities is associated with the tectonic movement, and stress changes. The changes in the meteorological and atmospheric parameters near the earth's surface associated with earthquakes are detected using multisatellite sensors, which provide information at the different pressure

levels [5], [14], [15]. The TOC over the epicentral region have shown characteristic features (increasing values) associated with earthquakes [39], [53].

The detection of anomalous signal associated with earthquakes is based on the multi-year background data as the definition of absolute local index of change of the environment (ALICE) proposed by Tramutoli [54], which and other derived methods have been successfully applied the detection of anomalous signals for different parameters associated with seismic [55]–[57], volcanic [58], [59], and dust storm events [60]. In the present article, we have used the data for the periods 2003–2020 (all available years covered 12 mo for AIRS data) as background data. The temporal mean value $\mu_t(x, y, p)$ and the standard deviation (STD) $\sigma_t(x, y, p)$ were computed using background data. $\mu_t(x, y, p)$ and $\sigma_t(x, y, p)$ are defined as follows:

$$\mu_t(x, y, p) = \frac{\sum_{i=1}^N O_{3-t}^{(i)}(x, y, p)}{N} \quad (1)$$

$$\sigma_t(x, y, p) = \sqrt{\frac{1}{N-1} \sum_{i=1}^N \left| O_{3-t}^{(i)}(x, y, p) - \mu_t(x, y, p) \right|^2} \quad (2)$$

where $O_{3-t}(x, y, p)$ is the ozone value at pressure level p located with latitude x and longitude y at the certain time (which can be different scales—hour, day, week, month, and here refers as day) observed by satellite. N is the number of the years with the background data. $\mu_t(x, y, p)$ and $\sigma_t(x, y, p)$ are the mean value and the STD of ozone for the certain day at pressure level p , latitude x and longitude y , respectively.

Further, we obtain the index of ozone variation (IOV) at different pressure levels with latitude x and longitude y defined as $S_t(x, y, p)$ using following equation:

$$S_t(x, y, p) = \frac{O_{3-t}(x, y, p) - \mu_t(x, y, p)}{\sigma_t(x, y, p)}. \quad (3)$$

The difference in IOV between every single day and the average value for 3 d prior is defined as $\bar{S}_t(x, y, p)$ in order to obtain the signals that differ from the variations in the adjacent days.

$$\bar{S}_t(x, y, p) = S_t(x, y, p) - \bar{S}_{\bar{t}}(x, y, p). \quad (4)$$

Here, $\bar{S}_{\bar{t}}(x, y, p)$ is the 3 d averaged IOV value prior to the certain day at pressure level p , latitude x , and longitude y .

Further, the index of ozone anomaly (IOA) defined as $\bar{S}_{t\Delta p}(x, y)$ is proposed, that is to focus on the unique variation both at the adjacent days in the same year and the same day in the different years, and also the difference between the lower troposphere and the upper troposphere.

$$\bar{S}_{t\Delta p}(x, y) = \bar{S}_t(x, y, p_l) - \bar{S}_t(x, y, p_u). \quad (5)$$

$\bar{S}_t(x, y, p_l)$ and $\bar{S}_t(x, y, p_u)$ are the IOV at the selected high pressure level (corresponds to lower altitude) and low pressure level (corresponds to higher altitude) in the troposphere based on the elevation of the target region, respectively. In the present study, we have considered ozone at 600 and 200 hPa pressure levels because the epicentral regions of the earthquakes are located at the high elevation, about 4000 m.

¹Online. [Available]: <https://www.livescience.com/17301-ozone-gas-earthquake-precursor-warning.html>

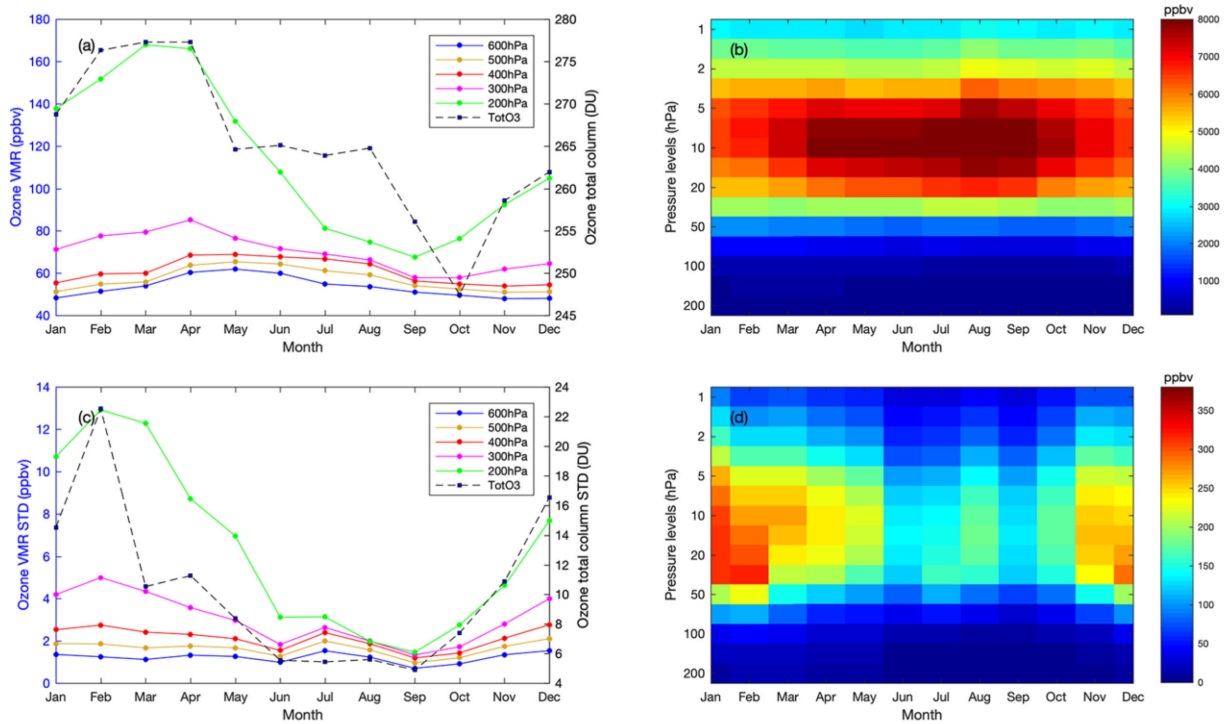


Fig. 1. Ozone monthly mean and STD variations of the epicenter region for Wenchuan earthquake during the period of 2003–2020. (a) O3 VMR mean variations in troposphere and TotO3. (b) O3 VMR mean variation in stratosphere. (c) O3 VMR STD variations in troposphere and TotO3. (d) O3 VMR STD variation in stratosphere.

III. RESULTS

A. Ozone Background Variations Over Epicentral Region

Considering the trend of tropospheric ozone varies highly with the different regions and seasons, and also the diurnal variability of ozone depends on solar radiations, complex terrain, and local precursor gas emissions [61], the nighttime ozone data over the pixel of the epicenter for the 2008 Wenchuan earthquake have been selected to study the background variations of ozone. The total integrated column ozone (TotO3) and O3 VMR at different pressure levels (600, 500, 400, 300, 200 hPa) have been considered in the present study due to the high elevation of the epicentral region.

The multiyear average monthly data were calculated by using the data for the periods 2003–2020. We have considered monthly ozone variations over the Wenchuan epicentral region (Fig. 1(a)). This clearly shows that the values of O3 VMR at 300 to 600 hPa pressure levels are much lower than the value at 200 hPa pressure level (the top of the troposphere). The maximum value of O3 VMR at 300–600 hPa pressure levels are observed in the month of April or May that could be related to the increased stratospheric–tropospheric exchange and photochemical processing in the middle latitudes of the northern hemisphere during spring season [62]. The variability in O3 VMR at 200 hPa could be associated with the seasonal variations. The maximum O₃ value at 200 hPa occurs in the month of March and the minimum value appears in the month of September. Variations of TotO3 [black dash line in Fig. 1(a)] show dependent on season, the maximum value appears in the month of April and the minimum in the month of October, mainly shows characteristic of

stratospheric ozone variations [the O3 VMR in the stratosphere is much higher compared to the troposphere, Fig. 1(b)]. We have computed the multiyear average monthly STD variations over the epicentral region of the Wenchuan earthquake during the periods 2003–2020. The higher STD values have been observed during winter season (January, February, and December) and the lower values in the month of September for every pressure level in the troposphere [Fig. 1(c)], which is similar to the mean ozone variations [Fig. 1(a)]. However, for the stratosphere, the highest O3 VMR STD variations occur during winter season compared to O3 VMR mean variations during autumn season [Fig. 1(d)].

B. Ozone Variations Associated With the 2008 Wenchuan *M* 7.8 Earthquake

We computed IOV using (3) at different pressure levels 200, 300, 400, 500 and 600 hPa in the troposphere over the epicentral region 60 d prior and after the Wenchuan earthquake using AIRS O3 VMR daily data (color map in Fig. 2). It is not easy to find the unusual signal. According to (5), IOA was computed (black line with red dots in Fig. 2). The IOA shows the highest IOA value of 3.723, 5 d prior to the earthquake (7 May, 2008). Further, we observed characteristic variations over the epicentral region during 366 d in 2008 [Fig. 3(a)], and also during the same period (April and May) from 2003 to 2020 [Fig. 3(b)]. In other words, the IOA shows distinctive variations prior to the Wenchuan earthquake compared with other days. In order to check whether this distinct variation only occurs over the epicentral area or exists in a wide area, we further obtained

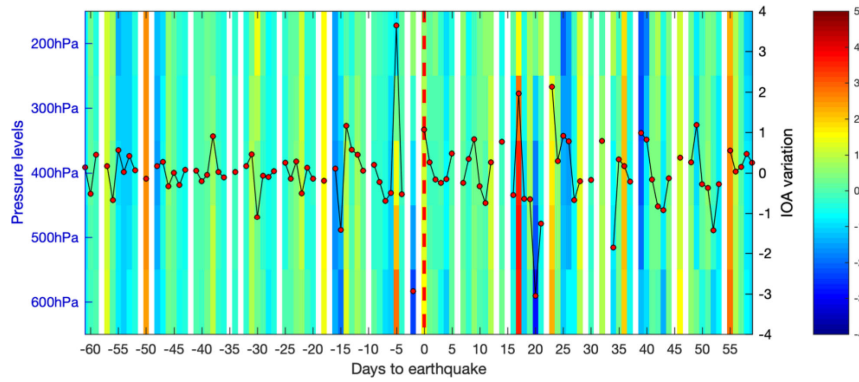


Fig. 2. Temporal variations of IOV at different pressure levels in troposphere and IOA over the epicentral region 60 d prior and after the Wenchuan earthquake. Black line shows IOA variation. Red dash line indicates the occurrence day of the main earthquake event.

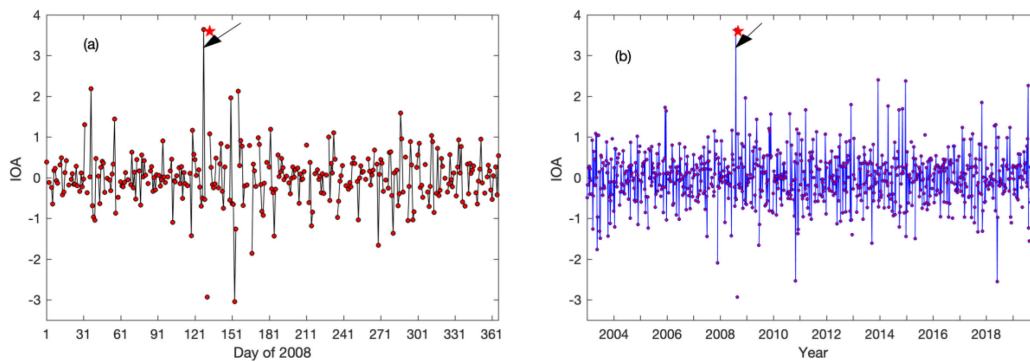


Fig. 3. Temporal variations of IOA over the epicentral region for the Wenchuan earthquake in (a) 2008 and (b) April and May during the periods 2003–2020. Red star indicates the day of earthquake occurrence. Black arrow shows the anomalous IOA variation.

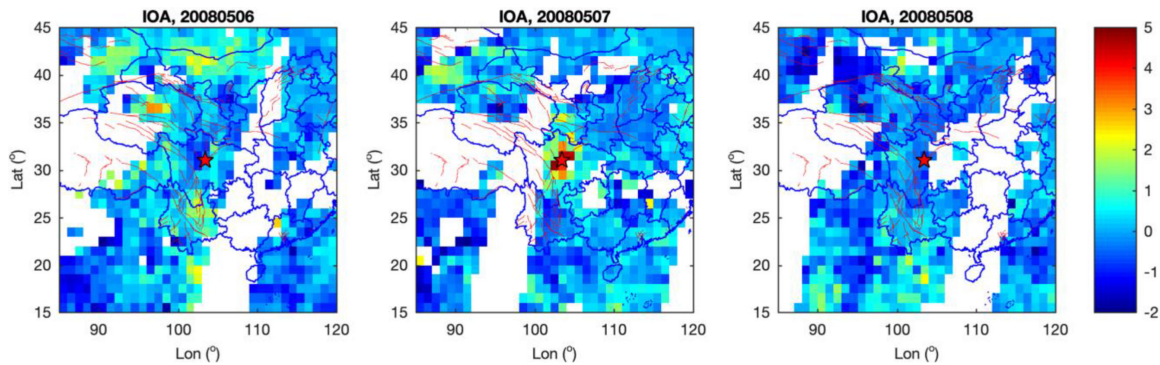


Fig. 4. Spatial variations of IOA on 6–8 May, 2008. Red star indicates the epicenter of the Wenchuan earthquake. Red lines show the main active faults in China. The region with white color shows gaps in data due to polar-orbiting satellite coverage.

the IOA spatial variations (Fig. 4), which show the distinct variations of IOA on 7 May 2008 over the epicentral region and distributed along the Longmenshan fault, the seismogenic fault of the Wenchuan earthquake. Both the temporal and spatial variations show an enhancement in tropospheric ozone 5 d prior to the main earthquake.

IV. DISCUSSION

To verify if the anomalous signal discussed in Section III is associated with the earthquake event, tropospheric ozone

variations around the time of another two strong earthquakes occurred in Sichuan province of China (the 2013 Lushan and the 2017 Jiuzhaigou earthquakes) have also been analyzed based on the method proposed in Section II-B. Additionally, considering the unusual variations of geophysical, hydrological, and geochemical parameters in the lithosphere, atmosphere, and ionosphere related to the Wenchuan earthquake based on ground and satellite observations have been reported by number of authors in [1], [7], [20], [33], [63], and [64], a possible mechanism of the observed tropospheric ozone variation is discussed in the next Section IV-B.

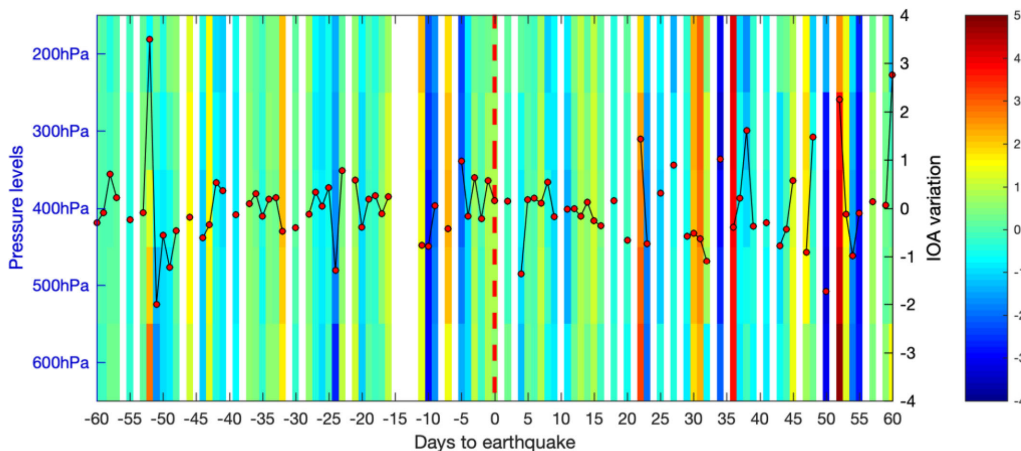


Fig. 5. Temporal variations of IOV at different pressure levels in the troposphere and IOA over the epicentral region 60 d prior and after the Lushan earthquake. Black line shows IOA variation. Red dash line indicates the day of earthquake occurrence.

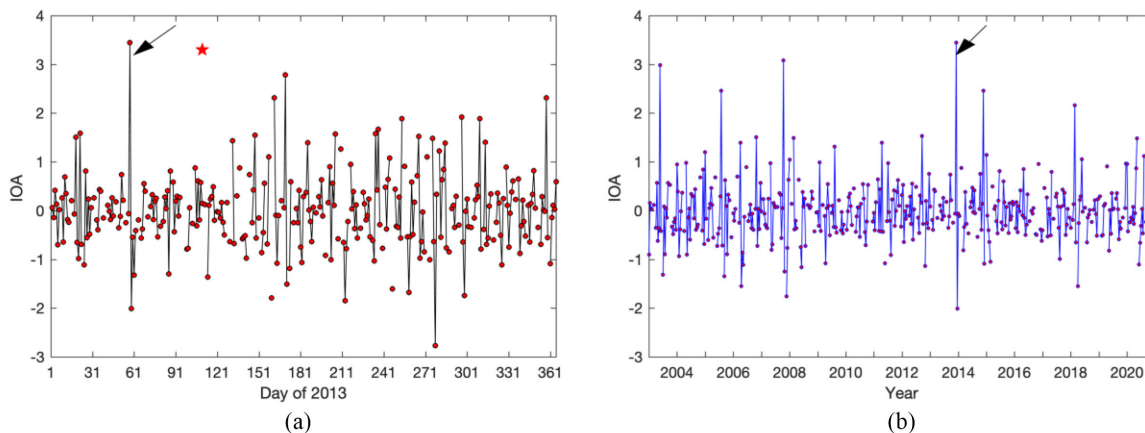


Fig. 6. Temporal variations of IOA over the epicentral region for the Lushan earthquake in (a) 2013 and (b) February during the periods 2003–2020. Red star indicates the day of earthquake occurrence. Black arrow shows the anomalous IOA variation.

A. Tropospheric Ozone Variations Associated With Other Strong Earthquakes Occurred in Sichuan Province

1) *2013 Lushan M6.6 Earthquake*: On 20 April 2013, the Lushan earthquake with the magnitude of 6.6 and the depth of 14 km (according to USGS) occurred on the Longmenshan fault zone, which is located about 80 km southwest of the 2008 Wenchuan earthquake. We processed the AIRS ozone data using the method described in Section II-B, and obtained the IOA time series variations over the epicentral region. From the IOA variations for 120 d (60 d prior and after the Lushan earthquake) (Fig. 5), an enhancement in IOA was observed 52 d prior to the earthquake event (27 February, 2013), which indicated an anomalous tropospheric ozone variation. Further, we studied the IOA variations throughout the whole year of 2013 [Fig. 6(a)] and for the month of February during the periods 2003 to 2020 [Fig. 6(b)], which clearly show the highest IOA variations on 27 February 2013 with the value of 3.445. From the spatial IOA variations (Fig. 7), we found an enhancement of IOA on 27 February 2013 over the epicentral area and over the southern part of Longmenshan fault.

Similar to the 2008 Wenchuan earthquake, an anomalous tropospheric ozone was observed prior to the Lushan earthquake over the epicenter and along the Longmenshan fault. But it appeared over 1 mo in advance instead of only a few days prior to the main earthquake event day in the case of Wenchuan earthquake. The enhancement in microwave brightness temperature, methane (CH_4), and carbon monoxide (CO) distributed along the Longmenshan fault have also been observed during the same period (over 1 mo prior to the main earthquake) for the 2013 Lushan earthquake [1], [20], which could be related to the existence of a large number of fractures along the Longmenshan fault and surrounding regions after the 2008 Wenchuan earthquake. The development of fractures during earthquake is likely to release gas from the near earth's surface due to changes in stress regime and also due to the changes in water level and radon emissions [64] prior to the Lushan earthquake. An enhancement in ozone 40 d prior to the earthquake has also been observed in Italy [39].

2) *2017 Jiuzhaigou M6.5 Earthquake*: On 8 August 2017, an earthquake with magnitude 6.5 with focal depth 9 km (according to USGS) hits the Jiuzhaigou, Sichuan province of China, which is another strong earthquake occurred on the eastern boundary of

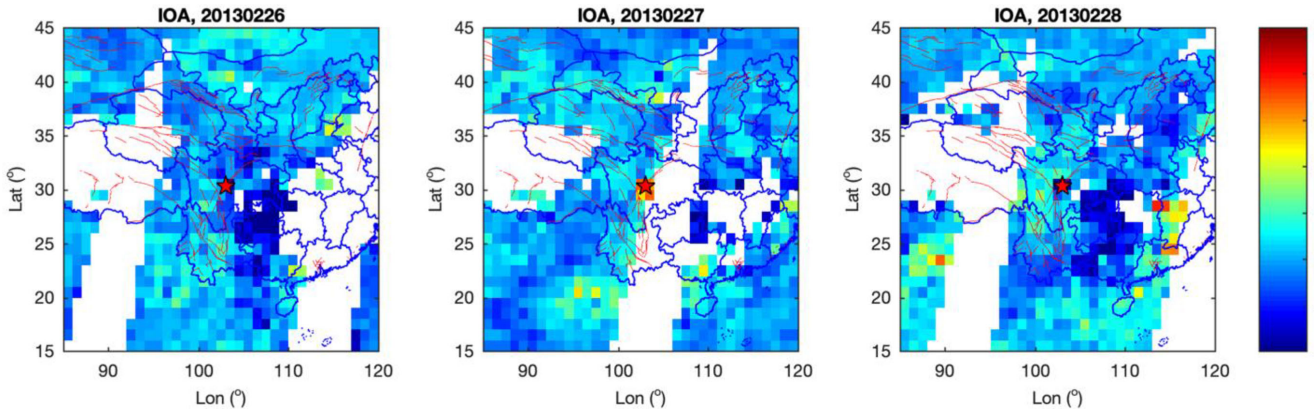


Fig. 7. Spatial variations of IOA on 26–28 February, 2013. Red star indicates epicenter of the Lushan earthquake. Red lines show the main active faults in China. The region with white color shows gaps in data due to polar-orbiting satellite coverage.

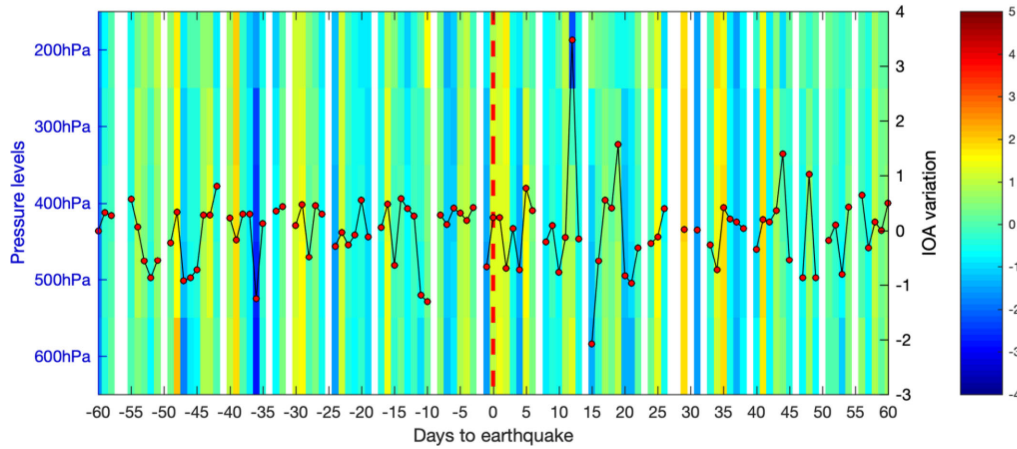


Fig. 8. Temporal variations of IOV at different pressure levels in troposphere and IOA over the epicentral region 60 d prior and after the Jiuzhaigou earthquake. Black line shows IOA variations. Red dash line indicates the day of earthquake event.

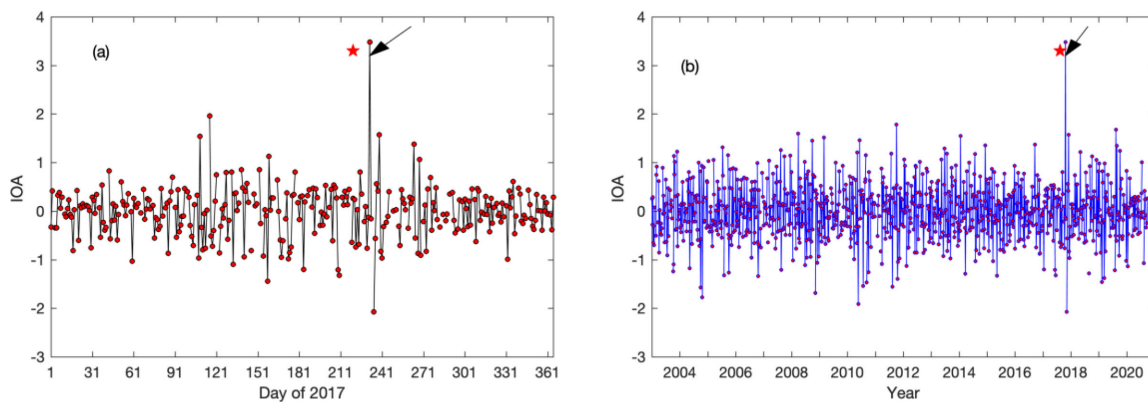


Fig. 9. Temporal variations of IOA over the epicentral region for the Jiuzhaigou earthquake in (a) 2017 and (b) July and August during the period 2003–2020. Red star indicates the day of earthquake occurrence. Black arrow shows the anomalous IOA variation.

the Bayan Har active block since the 2008 Wenchuan earthquake and the 2013 Lushan earthquake. This earthquake occurred on a left-lateral strike-slip fault [65]. The temporal variations of IOV at different pressure levels in troposphere and IOA over the epicentral region 60 d prior and after the Jiuzhaigou earthquake are shown in Fig. 8. The highest IOA value of 3.476 occurred on

the 13 d after the main earthquake event (20 August 2017), which was also the highest value during the year 2017 [Fig. 9(a)] and the same period (July and August) during 2003–2020 [Fig. 9(b)]. The spatial IOA variations from 19 to 21 August 2017 are shown in Fig. 10. An enhancement in IOA on 20 August has been observed over the epicentral region (Fig. 10). Unlike the anomalous

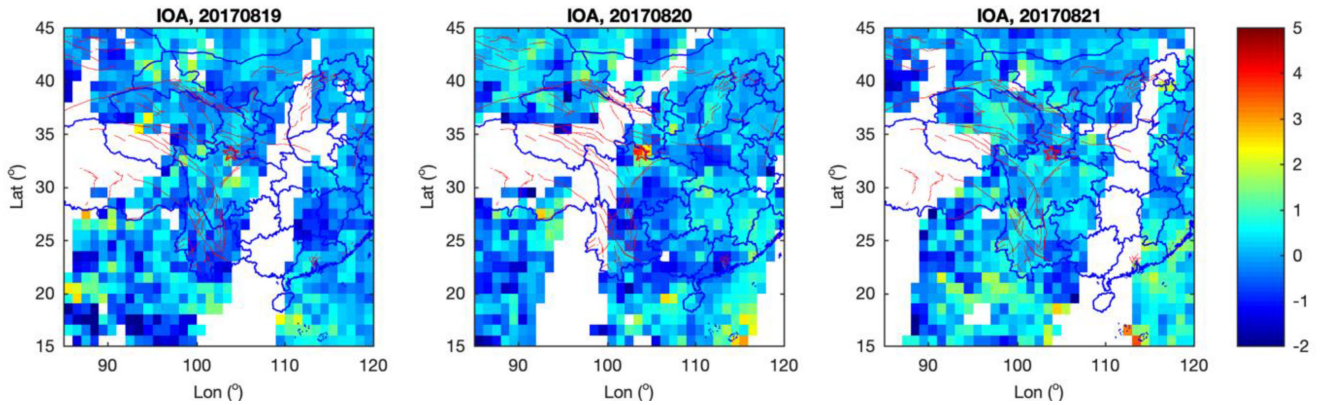


Fig. 10. Spatial variations of IOA on 19–21 August 2017. Red star indicates the epicenter of the Jiuzhaigou earthquake. Red lines show the main active faults in China. The region with white color shows gaps in data due to polar-orbiting satellite coverage.

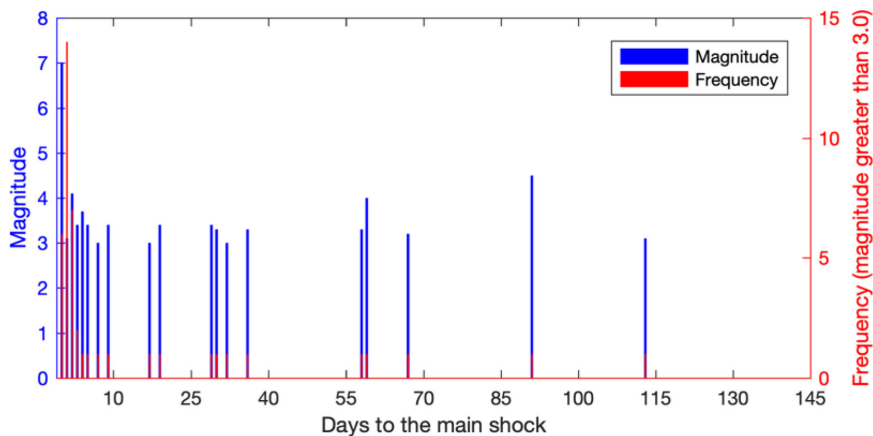


Fig. 11. Temporal distributions of the magnitude and frequency for the aftershocks with magnitude greater than 3.0 of the 2017 Jiuzhaigou earthquake (up to 31 December 2017), source earthquake catalog from China Earthquake Networks Center (CENC).

ozone variations appearing prior to the main earthquake event for the Wenchuan and the Lushan earthquakes, increase in IOA was observed after the Jiuzhaigou earthquake, which could be due to the presence of a blind fault that may not be source of gas emissions prior to the earthquake. It may be noted that the gas emissions depend on the geological and hydrological environment. The sudden changes in IOA after the Jiuzhaigou earthquake could be related to the microfracture caused by the main earthquake event and high frequency aftershock activities during one week after the main earthquake. From the temporal distributions of the magnitude and frequency for the aftershocks ($M > 3$) of the 2017 Jiuzhaigou earthquake (Fig. 11), we can see most of the aftershocks occurred within one week after the main earthquake event.

B. Possible Mechanism

In order to study the possible mechanism for the tropospheric ozone variations and the seismic coupling effect of the multi-sphere of the earth (lithosphere, atmosphere, and ionosphere), we collected the other parameters with unusual behaviors in different geospheres associated with the 2008 Wenchuan earthquake from the published research papers (Table I). It should be noted that almost all kinds of parameters have observed obvious

variations around 5 d before the main shock - 7 May 2008 (the occurrence day of the increased tropospheric ozone observed in the present article).

Our result is focused on the variations of tropospheric ozone instead of TOC mainly reflecting the stratospheric variations. An increase in tropospheric ozone occurred 5 d prior to the Wenchuan earthquake could be attributed to the following reasons.

1) Charge separation and electrical discharges in the lower atmosphere due to microfracture of rock and high electric fields induced by the stress accumulation is a possible reason for increased tropospheric ozone as provided by the experimental evidence [48] and the theoretical study [66]. That could be related to air ionization led by positive hole charge carriers [67] or increased radon emanation from the active faults, which lead to the vertical electric field generation. The increased water radon 1–2 weeks prior to the Wenchuan earthquake have been observed using ground-based data [64]. The ionospheric distributions have also been observed 3–6 d prior to the Wenchuan earthquake under the impact of a strong vertical electric field on the Earth's surface penetrating into the ionosphere [36], [37], [42], [43], [63]. The changes in electric field can also generate thermal radiation as the observed quasi-synchronous increase in some temperature-related parameters in the case of Wenchuan

TABLE I
OTHER PARAMETERS WITH ANOMALOUS BEHAVIORS AROUND THE TIME OF THE WENCHUAN EARTHQUAKE

| Parameter/Sensor | Altitude | Behavior | Days to earthquake | Source |
|---------------------------------------------|-------------|----------|----------------------------|---------------------|
| MBT ¹ (SSMIS) | Lithosphere | Increase | -12 to -8 | Jing et al.[1] |
| MBT ¹ (AMSR-E) | Lithosphere | Increase | -10, -7, -5, -1, 0, +4, +6 | Qi et al.[2] |
| SKT ² (NCEP) | Lithosphere | Increase | -6 | Wu et al.[8] |
| AP ³ (NCEP) | Atmosphere | Decrease | -10, -5 | Jing et al.[27] |
| SLHF ⁴ (NCEP) | Atmosphere | Increase | -1 | Jing et al.[27] |
| AT ⁵ and DTR ⁶ (NCEP) | Atmosphere | Increase | -6 | Wu et al.[8] |
| TotCO ⁷ (AIRS) | Atmosphere | Increase | -8, 0, +8 | Cui et al. [20] |
| CH ₄ VMR ⁸ (AIRS) | Atmosphere | Increase | -8 | Cui et al. [21] |
| AOD ⁹ (MODIS) | Atmosphere | Increase | -7 | Qin et al.[22] |
| RH ¹⁰ (AIRS) | Atmosphere | Decrease | -7 | Singh et al. [33] |
| OLR ¹¹ (NOAA) | Atmosphere | Increase | -7, -5, -1 | Jing et al.[27] |
| Clr-OLR ¹² (AIRS) | Atmosphere | Increase | -6, -5 | Wu et al.[8] |
| GPS TEC ¹³ | Ionosphere | Increase | -3 | Zhao et al.[36, 37] |
| Plasma (Demeter) | Ionosphere | Increase | -3 | Zhang et al.[42] |
| foF ₂ ¹⁴ (Ionosondes) | Ionosphere | Increase | -3 | Xu et al.[43] |

¹Microwave brightness temperature. ²Skin temperature. ³Air pressure. ⁴Surface latent heat flux. ⁵Air temperature. ⁶Diurnal temperature range. ⁷Total column CO. ⁸CH₄ volume mixing ratio. ⁹Aerosol optical depth. ¹⁰Relative humidity. ¹¹Outgoing longwave radiation. ¹²Clear-sky outgoing longwave radiation. ¹³Total electron content. ¹⁴Critical frequency of the F₂ layer.

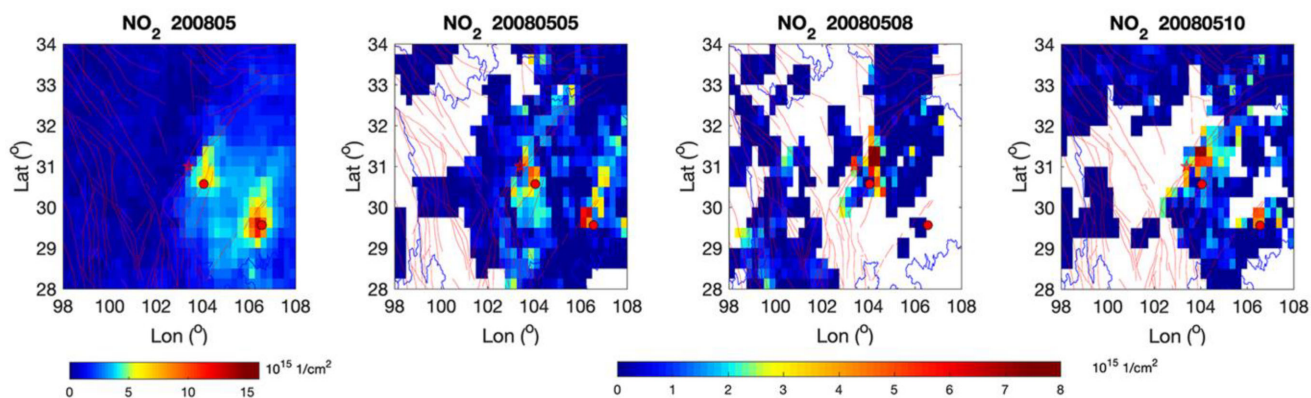


Fig. 12. Spatial variations of monthly-averaged NO₂ in May 2008 and daily NO₂ on 5, 8, and 10 May 2008 observed by OMI/Aura. Red star indicates the epicenter of the Wenchuan earthquake. Red dots show the main cities (Chengdu and Chongqing). Red lines show the main active faults in China. The region with white color shows no data available due to cloud screening.

earthquake, i.e., microwave brightness temperature (MBT) [1], [2], skin temperature (SKT) [8], air temperature (AT) [8], diurnal temperature range (DTR) [8], and outgoing longwave radiation (OLR) [27] (see Table I). Coseismic responses of groundwater level and temperature have also been observed [7], [68].

2) Increased ozone precursors around the time of earthquake occurrence. A large amount of CO and CH₄ emissions along the Longmenshan fault zone have been observed before the occurrence of the main shock [20], [21]. It should be noted that the high values in CO and CH₄ occurred 8 d before the earthquake, which seems 3 d earlier than the increased ozone we detected. However, the fact is these variations could be simultaneous due to the 8-d averaged data have been used in the analysis of CO and CH₄ [20], [21]. The details on the process of CO and CH₄ converting to ozone in the troposphere can be found in the reference [69]. As an important ozone precursor, the enhancement in tropospheric NO₂ (distracted from the monthly-averaged value) has been observed along the Longmenshan fault zone on 5, 8, and 10 May 2008 (around the day of increased tropospheric ozone) using OMI (onboard on the EOS-Aura satellite) data (Fig. 12),

which clearly shows those variations are not associated with the anthropogenic emissions located directly above the major urban areas of Chengdu and Chongqing (red dots in Fig. 12) as we observed in monthly-averaged NO₂ variation. In this case, it is more conducive to tropospheric ozone production under the photochemical and chemical reactions. The enhancement of NO₂ attribute to the release of nitrogen (N₂) along the active fault due to the change in stress [70]. Increased NO₂ associated with earthquakes has been observed in many earthquakes [53], [71].

3) The transport of ozone-rich air from the high latitude area and the lower stratosphere. We observed that the increase in tropospheric ozone and a sudden drop in air pressure have been observed on the same day (5 d prior to the main event) [27]. The low air pressure could disturb the wind pattern, thus forming favorable conditions for ozone enhancement as suggested by Ganguly [34], [41]. In addition, high temperature (MBT and SKT) and low relative humidity have been observed 6–7 d prior to the main earthquake event [1], [2], [8], [27], [33], which is also a favorable condition for ozone generation. The enhanced

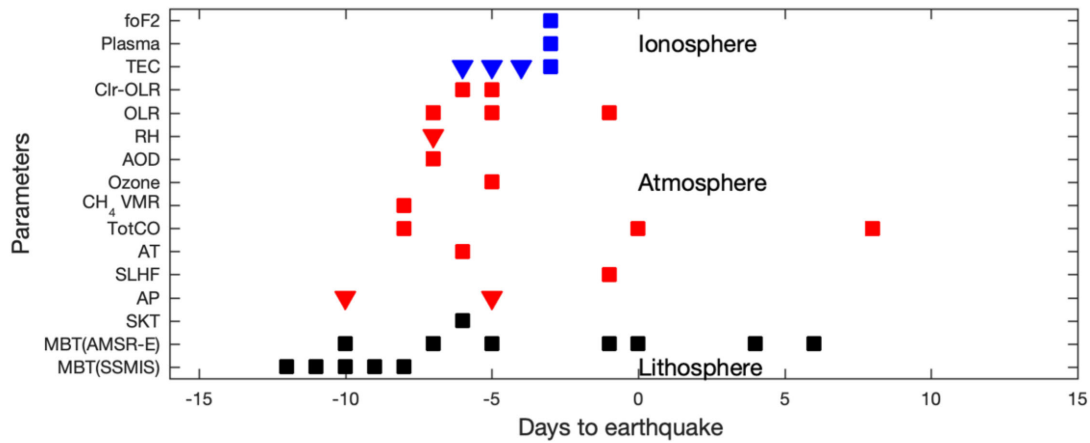


Fig. 13. Temporal distributions of multiparameter unusual variations around the day of Wenchuan earthquake based on the results of the present work and other published papers (details in Table I). Black markers indicate the lithospheric parameters; red markers indicate the atmospheric parameters; blue markers indicate the ionospheric parameters. Triangles represent decreased variations and squares represent the increased variations.

ozone following the increased SKT has also been observed in the Amatrice–Norcia earthquake sequence, Italy [39].

During the preparation stage of a strong earthquake, the enhancement in tropospheric ozone should be a comprehensive result related to the different factors we mentioned above instead of only one reason. The magnitude of earthquake could be one of the important factors to the appearance of the anomalous tropospheric ozone. Our results clearly show that the range of spatial distribution and the value of IOA will increase with the magnitude of earthquakes, and vice versa. The occurrence time of increased tropospheric ozone depends on the tectonic environment, focal mechanism, and weather conditions as suggested by the results of the Lushan and Jiuzhaigou earthquakes (Section IV-A).

The temporal distributions of multiparameter variations around the occurrence of the 2008 Wenchuan earthquake are shown in Fig. 13, that will help us understand the interaction of the parameters with anomalous behaviors at different altitudes during the period of earthquake preparation. The parameters listed on the y-axis in Fig. 13 are arranged according to their vertical heights. The parameters at the bottom reflect the variations coming from lithosphere, and those at the top are coming from the ionosphere. It is easy to find the appearance of the unusual behaviors from lithosphere to upper atmosphere (ionosphere) is gradually approaching the day of earthquake occurrence. Similar phenomenon has been observed in the 2015 Nepal earthquake [14]. The earliest anomalies occurred in the lithosphere and the impending signals occurred in the mid to upper atmosphere (ionosphere) follow the bottom-up pattern that can be explained by the root of these variations is the stress accumulation coming from the earth's crust. Air ionization produced by radon emission is considered a main source for the coupling effect of lithosphere and atmosphere during the preparation phase of earthquake as suggested by the LAIC model [28]. A series of thermal-related parameters show changes due to air ionization and gases emission (Fig. 13) (e.g., CO, CO₂, CH₄, etc.) in the epicentral region [72]. Quasi synchronous change in aerosols and ozone could appear during this period under the comprehensive influence of many factors, as observed in the 2008 Wenchuan earthquake

([22] and present work) and the 2015 Nepal earthquake [53], and also after the earthquake occurrence [41], [73]. Further, the ionosphere will be affected by the changes in atmospheric conductivity and lead to the variations in the ionosphere, e.g., TEC, foF2, plasma, etc.

V. CONCLUSION

Our results show variations of tropospheric ozone associated with the 2008 Wenchuan earthquake. The IOA based on AIRS data for an 18-year period (2003 to 2020) show a distinct increase in the tropospheric ozone observed 5 d prior to the main earthquake event. The location of enhanced tropospheric ozone is consistent with the epicenter for the impending earthquake, and also distributed along the Longmenshan fault zone. The reason for unusual behavior in the tropospheric ozone could be related to charge separation and electrical discharges, increased ozone precursors, and intrusion of high concentration ozone in the stratosphere, etc. The magnitude of earthquake could be an important factor affecting the appearance of the anomalous tropospheric ozone. The occurrence time of increased tropospheric ozone depends on the tectonic environment, focal mechanism, weather conditions, and so on. The strong coupling has been observed among the lithosphere, the atmosphere, and the ionosphere around the day of increased tropospheric ozone, which could be supported by the LAIC model proposed by Pulinet and Ouzounov [28].

It should be noted that the possible anomalous signals associated with earthquakes could differ from place to place due to the difference in seismogenic environments (e.g., magnitude, depth, location, focal mechanism, fault locking status, geological, geophysical, tectonic and hydrological environment, etc.), and also with the atmospheric perturbations (such as dust storms, extreme events, volcanic eruptions, forest fires/biomass burning, cyclones/typhoons/hurricanes, etc.). The statistical analysis is difficult to carry out due to lack of repeatable earthquake in similar geological, geophysical and hydrological environment. Combined with multiparameter in different geospheres could

be a more practical approach to identify the anomalous signals associated with earthquake activities [39].

ACKNOWLEDGMENT

The authors would like to thank NASA's Goddard Earth Sciences Data and Information Services Center (GES DISC) for AIRS and OMI/Aura dataset archived and distributed. They would also thank the anonymous reviewers for their comments/suggestions that have helped them to improve earlier versions of the manuscript.

REFERENCES

- [1] F. Jing, R. P. Singh, Y. Cui, and K. Sun, "Microwave brightness temperature characteristics of three strong earthquakes in sichuan province, china," *IEEE J. Sel. Topics Appl. Earth Observ. Remote Sens.*, vol. 13, pp. 513–522, 2020.
- [2] Y. Qi, L. Wu, M. He, and W. Mao, "Spatio-temporally weighted two-step method for retrieving seismic MBT anomaly: May 2008 Wenchuan earthquake sequence being a case," *IEEE J. Sel. Topics Appl. Earth Observ. Remote Sens.*, vol. 13, pp. 382–391, Jan. 2020.
- [3] S. Hsu *et al.*, "Evaluating real-time air-quality data as earthquake indicator," *Sci. Total Environ.*, vol. 408, no. 11, pp. 2299–2304, 2010.
- [4] K. Wallace, R. Bilham, F. Blume, V. K. Gaur, and V. K. Gahalaut, "Geodetic constraints on the Bhuj 2001 earthquake and surface deformation in the Kachchh rift basin," *Geophysical Res. Lett.*, vol. 33, no. 10, 2006.
- [5] R. P. Singh, J. S. Kumar, J. Zlotnicki, and M. Kafatos, "Satellite detection of carbon monoxide emission prior to the Gujarat earthquake of 26 January 2001," *Appl. Geochemistry*, vol. 25, no. 4, pp. 580–585, 2010.
- [6] A. A. Tronin, P. F. Biagi, O. A. Molchanov, Y. M. Khatkevich, and E. I. Gordeev, "Temperature variations related to earthquakes from simultaneous observation at the ground stations and by satellites in Kamchatka area," *Phys. Chem. Earth*, vol. 29, no. 4, pp. 501–506, 2004.
- [7] A. He and R. P. Singh, "Groundwater level response to the Wenchuan earthquake of May 2008," *Geomatics, Natural Hazards Risk*, vol. 10, no. 1, pp. 336–352, 2019.
- [8] L. Wu, K. Qin, and S. Liu, "GEOSS-based thermal parameters analysis for earthquake anomaly recognition," *Proc. IEEE*, vol. 100, no. 10, pp. 2891–2907, Oct. 2012.
- [9] S. A. Pulnits *et al.*, "Thermal, atmospheric and ionospheric anomalies around the time of the Colima M7.8 earthquake of 21 January 2003," *Annales Geophysicae*, vol. 24, no. 3, pp. 835–849, 2006.
- [10] P. F. Biagi *et al.*, "LF radio anomalies revealed in Italy by the wavelet analysis: Possible preseismic effects during 1997–1998," *Phys. Chem. Earth*, vol. 31, no. 4, pp. 403–408, 2006.
- [11] D. Marchetti *et al.*, "Possible lithosphere-atmosphere-ionosphere coupling effects prior to the 2018 MW = 7.5 Indonesia earthquake from seismic, atmospheric and ionospheric data," *J. Asian Earth Sci.*, vol. 188, 2020, Art. no. 104097.
- [12] L. Wu *et al.*, "Geosphere coupling and hydrothermal anomalies before the 2009 MW 6.3 L'Aquila earthquake in Italy," *Natural Hazards Earth Syst. Sci.*, vol. 16, pp. 1859–1880, 2016.
- [13] M. Akhoondzadeh, A. De Santis, D. Marchetti, A. Piscini, and S. Jin, "Anomalous seismo-LAI variations potentially associated with the 2017 MW = 7.3 Sarpol-e-Zahab (Iran) earthquake from swarm satellites, GPS-TEC and climatological data," *Adv. Space Res.*, vol. 64, no. 1, pp. 143–158, 2019.
- [14] F. Jing, R. P. Singh, and X. Shen, "Land-atmosphere-meteorological coupling associated with the 2015 Gorkha (M 7.8) and Dolakha (M 7.3) Nepal earthquakes," *Geomatics, Natural Hazards Risk*, vol. 10, no. 1, pp. 1267–1284, 2019.
- [15] R. P. Singh, W. Mehdi, and M. Sharma, "Complementary nature of surface and atmospheric parameters associated with Haiti earthquake of 12 January 2010," *Natural Hazards Earth Syst. Sci.*, vol. 10, no. 6, pp. 1299–1305, 2010.
- [16] Y. Qi, L. Wu, W. Mao, Y. Ding, and M. He, "Discriminating possible causes of microwave brightness temperature positive anomalies related with May 2008 Wenchuan earthquake sequence," *IEEE Trans. Geosci. Remote Sens.*, vol. 59, no. 3 pp. 1–14, Mar. 2020.
- [17] A. A. Tronin, M. Hayakawa, and O. A. Molchanov, "Thermal IR satellite data application for earthquake research in Japan and China," *J. Geodynamics*, vol. 33, no. 4/5, pp. 519–534, 2002.
- [18] D. Ouzounov, N. Bryant, T. Logan, S. Pulnits, and P. Taylor, "Satellite thermal IR phenomena associated with some of the major earthquakes in 1999–2003," *Phys. Chem. Earth Parts A/b/c*, vol. 31, no. 4–9, pp. 154–163, 2006.
- [19] V. Tramutoli *et al.*, "On the possible origin of thermal infrared radiation (TIR) anomalies in earthquake-prone areas observed using robust satellite techniques (RST)," *Chem. Geol.*, vol. 339, no. 2, pp. 157–168, 2013.
- [20] Y. Cui, D. Ouzounov, N. Hatzopoulos, K. Sun, Z. Zou, and J. Du, "Satellite observation of CH₄ and CO anomalies associated with the Wenchuan MS 8.0 and Lushan MS 7.0 earthquakes in China," *Chem. Geol.*, vol. 469, pp. 185–191, 2017.
- [21] J. Cui, X. Shen, J. Zhang, W. Ma, and W. Chu, "Analysis of spatiotemporal variations in middle-tropospheric to upper-tropospheric methane during the Wenchuan Ms = 8.0 earthquake by three indices," *Nat. Hazards Earth Syst. Sci.*, vol. 19, no. 12, pp. 2841–2854, 2019.
- [22] K. Qin, L. X. Wu, S. Zheng, Y. Bai, and X. Lv, "Is there an abnormal enhancement of atmospheric aerosol before the 2008 Wenchuan earthquake?," *Adv. Space Res.*, vol. 54, no. 6, pp. 1029–1034, 2014.
- [23] Q. Liu, A. De Santis, A. Piscini, G. Cianchini, G. Ventura, and X. Shen, "Multi-parametric climatological analysis reveals the involvement of fluids in the preparation phase of the 2008 Ms 8.0 Wenchuan and 2013 Ms 7.0 Lushan earthquakes," *Remote Sens.*, vol. 12, no. 10, 2020, Art. no. 1663.
- [24] J. Y. Liu *et al.*, "A spatial analysis on seismo-ionospheric anomalies observed by DEMETER during the 2008 M8.0 Wenchuan earthquake," *J. Asian Earth Sci.*, vol. 114, no. 2, pp. 414–419, 2015.
- [25] J. Błęcki, M. Parrot, and R. Wronowski, "Plasma turbulence in the ionosphere prior to earthquakes, some remarks on the DEMETER registrations," *J. Asian Earth Sci.*, vol. 41, no. 4, pp. 450–458, 2011.
- [26] Z. Zhima *et al.*, "Possible ionospheric electromagnetic perturbations induced by the Ms7.1 Yushu earthquake," *Earth Moon Planets*, vol. 108, no. 3, pp. 231–241, 2012.
- [27] F. Jing, X. H. Shen, C. L. Kang, and P. Xiong, "Variations of multi-parameter observations in atmosphere related to earthquake," *Natural Hazards Earth Syst. Sci.*, vol. 13, no. 1, pp. 27–33, 2013.
- [28] S. Pulnits and D. Ouzounov, "Lithosphere-atmosphere-ionosphere coupling (LAIC) model—An unified concept for earthquake precursors validation," *J. Asian Earth Sci.*, vol. 41, pp. 371–382, 2011.
- [29] V. A. Liperovsky, O. A. Pokhotelov, C. V. Meister, and E. V. Liperovskaya, "Physical models of coupling in the lithosphere-atmosphere-ionosphere system before earthquakes," *Geomagnetism Aeronomy*, vol. 48, no. 6, pp. 795–806, 2008.
- [30] S. Zheng and R. Singh, "Aerosol and meteorological parameters associated with the intense dust event of 15 April 2015 over Beijing, China," *Remote Sens.*, vol. 10, no. 6, 2018, Art. no. 957.
- [31] F. Jing, A. Chauhan, R. P. Singh, and P. Dash, "Changes in atmospheric, meteorological, and ocean parameters associated with the 12 January 2020 Taal volcanic eruption," *Remote Sens.*, vol. 12, no. 6, 2020, Art. no. 1026.
- [32] V. V. Lasukov, "Ozone, percolation, and aerosol mechanisms of an electromagnetic earthquake predictor," *Russian Phys. J.*, vol. 43, no. 2, pp. 143–148, 2000.
- [33] R. P. Singh, W. Mehdi, R. Gautam, J. Senthil Kumar, J. Zlotnicki, and M. Kafatos, "Precursory signals using satellite and ground data associated with the Wenchuan earthquake of 12 May 2008," *Int. J. Remote Sens.*, vol. 31, no. 13, pp. 3341–3354, 2010.
- [34] N. D. Ganguly, "Variation in atmospheric ozone concentration following strong earthquakes," *Int. J. Remote Sens.*, vol. 30, no. 2, pp. 349–356, 2009.
- [35] A. Amani, S. Mansor, B. Pradhan, L. Billa, and S. Pirasteh, "Coupling effect of ozone column and atmospheric infrared sounder data reveal evidence of earthquake precursor phenomena of Bam earthquake, Iran," *Arabian J. Geosciences*, vol. 7, no. 4, pp. 1517–1527, 2014.
- [36] B. Zhao *et al.*, "Is an unusual large enhancement of ionospheric electron density linked with the 2008 great Wenchuan earthquake?," *J. Geophysical Res.: Space Phys.*, vol. 113, 2008, Art. no. A11304.
- [37] B. Zhao, M. Wang, T. Yu, G. Xu, W. Wan, and L. Liu, "Ionospheric total electron content variations prior to the 2008 Wenchuan earthquake," *Int. J. Remote Sens.*, vol. 31, pp. 3545–3557, 2010.
- [38] A. Tertyshnikov, "The variations of ozone content in the atmosphere above strong earthquake epicenter," *Izvestiya Phys. Solid Earth*, vol. 31, pp. 789–794, 1995.
- [39] A. Piscini, A. De Santis, D. Marchetti, and G. Cianchini, "A Multi-parametric climatological approach to study the 2016 Amatrice–Norcia (Central Italy) earthquake preparatory phase," *Pure Appl. Geophys.*, vol. 174, no. 10, pp. 3673–3688, Oct. 2017.

- [40] A. Tronin, "Remote sensing and earthquakes: A review," *Phys. Chem. Earth*, vol. 31, no. 4–9, pp. 138–142, 2006.
- [41] N. D. Ganguly, "The impact of transported ozone-rich air on the atmospheric ozone content following the 26 January 2001 and 7 March 2006 Gujarat earthquakes," *Remote Sens. Lett.*, vol. 2, no. 3, pp. 195–202, 2011.
- [42] X. Zhang, X. Shen, J. Liu, X. Ouyang, J. Qian, and S. Zhao, "Analysis of ionospheric plasma perturbations before Wenchuan earthquake," *Natural Hazards Earth Syst. Sci.*, vol. 9, pp. 1259–1266, 2009.
- [43] T. Xu, Y. Hu, J. Wu, Z. Wu, Y. Suo, and J. Feng, "Giant disturbance in the ionospheric F2 region prior to the M 8.0 Wenchuan earthquake on 12 May 2008," *Annales Geophysicae*, vol. 28, pp. 1533–1538, 2010.
- [44] P. Xiong *et al.*, "Towards advancing the earthquake forecasting by machine learning of satellite data," *Sci. Total Environ.*, vol. 771, 2021, Art. no. 145256.
- [45] M. N. Efstathiou, "A case study of the association of total ozone variability with major earthquakes in Greece during 2001–2010," *Remote Sens. Lett.*, vol. 3, no. 3, pp. 181–190, 2012.
- [46] E. Dologlou, "On the possibility of total ozone variability as a precursor for major earthquakes in Greece," *Remote Sens. Lett.*, vol. 4, no. 3, pp. 237–242, 2013.
- [47] C. A. Varotsos, M. N. Efstathiou, and A. P. Cracknell, "On the association of aerosol optical depth and total ozone fluctuations with recent earthquakes in Greece," *Acta Geophysica*, vol. 65, no. 4, pp. 659–665, 2017.
- [48] R. A. Baragiola, C. A. Dukes, and D. Hedges, "Ozone generation by rock fracture: Earthquake early warning?," *Appl. Phys. Lett.*, vol. 99, no. 20, 2011, Art. no. 204101.
- [49] J. Fishman and P. J. Crutzen, "The origin of ozone in the troposphere," *Nature*, vol. 274, no. 5674, pp. 855–858, 1978.
- [50] X. Lu *et al.*, "Exploring 2016–2017 surface ozone pollution over China: Source contributions and meteorological influences," *Atmospheric Chem. Phys.*, vol. 19, no. 12, pp. 8339–8361, 2019.
- [51] J. Susskind, J. Blaisdell, and L. Iredell, "Improved methodology for surface and atmospheric soundings, error estimates, and quality control procedures: The atmospheric infrared sounder science team version-6 retrieval algorithm," *J. Appl. Remote Sens.*, vol. 8, no. 1, 2014, Art. no. 084994.
- [52] B. H. Kahn *et al.*, "The atmospheric infrared sounder version 6 cloud products," *Atmos. Chem. Phys.*, vol. 14, no. 1, pp. 399–426, 2014.
- [53] N. D. Ganguly, "Atmospheric changes observed during April 2015 Nepal earthquake," *J. Atmospheric Sol.-Terr. Phys.*, vol. 140, pp. 16–22, 2016.
- [54] V. Tramutoli, "Robust AVHRR techniques (RAT) for environmental monitoring: Theory and applications," *Earth Surf. Remote Sens. II*, vol. 3496, pp. 101–113, 1998.
- [55] R. Corrado, R. Caputo, C. Filizzola, N. Pergola, C. Pietrapertosa, and V. Tramutoli, "Seismically active area monitoring by robust TIR satellite techniques: A sensitivity analysis on low magnitude earthquakes in Greece and Turkey," *Natural Hazards Earth Syst. Sci.*, vol. 5, no. 1, pp. 101–108, 2005.
- [56] N. Pergola *et al.*, "Using RST approach and EOS-MODIS radiances for monitoring seismically active regions: A study on the 6 April 2009 Abruzzo earthquake," *Natural Hazards Earth Syst. Sci.*, vol. 10, no. 2, pp. 239–249, 2010.
- [57] F. Jing, R. P. Singh, K. Sun, and X. Shen, "Passive microwave response associated with two main earthquakes in Tibetan plateau, China," *Adv. Space Res.*, vol. 62, no. 7, pp. 1675–1689, 2018.
- [58] F. Marchese, A. Falconieri, N. Pergola, and V. Tramutoli, "A retrospective analysis of the Shinmoedake (Japan) eruption of 26–27 January 2011 by means of Japanese geostationary satellite data," *J. Volcanol. Geothermal Res.*, vol. 269, pp. 1–13, 2014.
- [59] F. Marchese, T. Lacava, N. Pergola, K. Hattori, E. Miraglia, and V. Tramutoli, "Inferring phases of thermal unrest at Mt. Asama (Japan) from infrared satellite observations," *J. Volcanol. Geothermal Res.*, vol. 237–238, pp. 10–18, 2012.
- [60] M. Francesco, S. Filomena, F. Alfredo, F. Carolina, P. Nicola, and T. Valerio, "An enhanced satellite-based algorithm for detecting and tracking dust outbreaks by means of SEVIRI data," *Remote Sens.*, vol. 9, no. 6, pp. 537, 2017.
- [61] S. Zhao, Y. Yu, D. Yin, D. Qin, J. He, and L. Dong, "Spatial patterns and temporal variations of six criteria air pollutants during 2015 to 2017 in the city clusters of Sichuan basin, China," *Sci. Total Environ.*, vol. 624, pp. 540–557, 2018.
- [62] P. S. Monks, "A review of the observations and origins of the spring ozone maximum," *Atmospheric Environ.*, vol. 34, no. 21, pp. 3545–3561, 2000.
- [63] J. Y. Liu *et al.*, "Seismoionospheric GPS total electron content anomalies observed before the 12 May 2008 Mw7.9 Wenchuan earthquake," *J. Geophysical Res., Space Phys.*, vol. 114, 2009, Art. no. A04320.
- [64] Q. Ye, R. P. Singh, A. He, S. Ji, and C. Liu, "Characteristic behavior of water radon associated with Wenchuan and Lushan earthquakes along Longmenshan fault," *Radiat. Meas.*, vol. 76, pp. 44–53, 2015.
- [65] D. Zhao, C. Qu, X. Shan, W. Gong, Y. Zhang, and G. Zhang, "InSAR and GPS derived coseismic deformation and fault model of the 2017 Ms7.0 Jiuzhaigou earthquake in the Northeast Bayanhar block," *Tectonophysics*, vol. 726, pp. 86–99, 2018.
- [66] V. Sorokin and Y. Y. Ruzhin, "Electrodynamic model of atmospheric and ionospheric processes on the eve of an earthquake," *Geomagnetism Aeronomy*, vol. 55, no. 5, pp. 626–642, 2015.
- [67] F. Freund, "Pre-earthquake signals: Underlying physical processes," *J. Asian Earth Sci.*, vol. 41, pp. 383–400, 2011.
- [68] A. He and R. P. Singh, "Coseismic groundwater temperature response associated with the Wenchuan earthquake," *Pure Appl. Geophys.*, vol. 177, no. 1, pp. 109–120, 2020.
- [69] J. Fishman, S. Solomon, and P. J. Crutzen, "Observational and theoretical evidence in support of a significant in-situ photochemical source of tropospheric ozone," *Tellus*, vol. 31, no. 5, pp. 432–446, 1979.
- [70] V. Walia *et al.*, "Geochemical variation of soil–gas composition for fault trace and earthquake precursory studies along the Hsincheng fault in NW Taiwan," *Appl. Radiat. Isot.*, vol. 67, pp. 1855–1863, 2009.
- [71] M. Shah, M. A. Tariq, and N. A. Naqvi, "Atmospheric anomalies associated with Mw>6.0 earthquakes in Pakistan and Iran during 2010–2017," *J. Atmospheric Sol.-Terr. Phys.*, vol. 191, 2019, Art. no. 105056.
- [72] V. Liperovsky, C.-V. Meister, E. Liperovskaya, V. Davidov, and V. Bogdanov, "On the possible influence of radon and aerosol injection on the atmosphere and ionosphere before earthquakes," *Natural Hazards Earth Syst. Sci.*, vol. 5, no. 6, pp. 783–789, 2005.
- [73] Y. Okada, S. Mukai, and R. Singh, "Changes in atmospheric aerosol parameters after Gujarat earthquake of January 26, 2001," *Adv. Space Res.*, vol. 33, no. 3, pp. 254–258, 2004.



Feng Jing (Member, IEEE) was born in 1979. She received the B.S. degree in geology from China University of Geosciences, Wuhan, China, the M.E. degree in geophysical prospecting and information technology from China University of Geosciences, Beijing, China, and the Ph.D. degree in cartography and geographic information system from the Institute of Remote Sensing Applications, Chinese Academy of Science, Beijing, China, in 2002, 2005, and 2010, respectively.

She is currently a Professor with the Institute of Earthquake Forecasting, China Earthquake Administration, Beijing, China. She is the author of two books and more than 20 papers. Her research interests include earthquake monitoring using remote sensing and lithosphere–atmosphere coupling associated with earthquakes.



Ramesh P. Singh (Senior Member, IEEE) received B.S. (Hons.) in 1974, M.Sc. and Ph.D. degrees in geophysics, in 1976 and 1980, respectively, from Banaras Hindu University, India.

He is currently a Professor with the Schmid College of Science and Technology, Chapman University, Orange, CA, USA. He was also a Professor with the Indian Institute of Technology, Kanpur, India, from 1986 to 2007, and George Mason University, Fairfax, VA, USA, from 2003 to 2005 and 2007 to 2009. He is the author of more than 250 papers. His research interests include natural hazards, early warning of coastal earthquakes, soil moisture, landslides, snow avalanches, floods, dust storms, remote sensing applications, geophysical explorations, atmospheric pollution, and mining environment.

Dr. Singh is the Chief Editor of the journal *Geomatics, Natural Hazards and Risk* published by Taylor and Francis, U.K.